Evidence that vitamin D₃ promotes mast cell-dependent reduction of chronic UVB-induced skin pathology in mice

Lisa Biggs,¹ Chunping Yu,^{1,2} Boris Fedoric,¹ Angel F. Lopez,^{1,2} Stephen J. Galli,³ and Michele A. Grimbaldeston^{1,2}

Mast cell production of interleukin-10 (IL-10) can limit the skin pathology induced by chronic low-dose ultraviolet (UV)-B irradiation. Although the mechanism that promotes mast cell IL-10 production in this setting is unknown, exposure of the skin to UVB irradiation induces increased production of the immune modifying agent 1α,25-dihydroxyvitamin D_3 ($1\alpha_125[OH]_2D_3$). We now show that $1\alpha_125(OH)_2D_3$ can up-regulate IL-10 mRNA expression and induce IL-10 secretion in mouse mast cells in vitro. To investigate the roles of $1\alpha,25(OH)_2D_3$ and mast cell vitamin D receptor (VDR) expression in chronically UVBirradiated skin in vivo, we engrafted the skin of genetically mast cell-deficient WBB6F1-Kit^{W/W-v} mice with bone marrow-derived cultured mast cells derived from C57BL/6 wild-type or VDR^{-/-} mice. Optimal mast cell-dependent suppression of the inflammation, local production of proinflammatory cytokines, epidermal hyperplasia, and epidermal ulceration associated with chronic UVB irradiation of the skin in KitW/W-v mice required expression of VDR by the adoptively transferred mast cells. Our findings suggest that 1α,25(OH)₂D₃/VDR-dependent induction of IL-10 production by cutaneous mast cells can contribute to the mast cell's ability to suppress inflammation and skin pathology at sites of chronic UVB irradiation.

CORRESPONDENCE
Michele Grimbaldeston:
michele.grimbaldeston@
health.sa.gov.au
OR
Stephen J. Galli:
sqalli@stanford.edu

The Journal of Experimental Medicine

Abbreviations used: $1\alpha,25(OH)_2D_3$, $1\alpha,25$ -dihydroxyvitamin D_3 ; BMCMC, BM-derived cultured mast cell; i.d., intradermal; VDR, vitamin D receptor.

In humans and mice, chronic UVB irradiation (wavelengths; 290–320 nm) induces cutaneous inflammation, photoaging, and gene mutations that can lead to the development of malignancies at affected sites (Kligman, 1996; Melnikova and Ananthaswamy, 2005). Although factors that promote UV-induced innate responses have been investigated intensively (Melnikova and Ananthaswamy, 2005), less is known about regulatory mechanisms that can limit UVB-induced inflammation.

Although mast cells were once thought to function primarily as proinflammatory effector cells that can contribute to either allergic reactions (Galli et al., 2005) or inflammation caused by innate responses to exogenous environmental agents such as UV irradiation (Metz et al., 2006), recent evidence indicates that, in certain settings, mast cells can also limit inflammation and tissue injury, including that induced by

UVB irradiation (Grimbaldeston et al., 2007; Galli et al., 2008). Mast cells are well positioned to participate in cutaneous immune responses, as skin mast cells are located predominately in the dermis near blood and lymphatic vessels and nerves. Although the majority of UVB rays do not penetrate to the dermis (Noonan and De Fabo, 1992), the UVB-dependent activation of dermal mast cells is thought to be achieved indirectly, e.g., via nerve growth factor derived from the epidermis (Hart et al., 2002; Townley et al., 2002) or by sensory C fibers (which innervate the epidermis and extend into the dermis) that have been activated by cis-urocanic acid (Hart et al., 1999, 2002; Khalil et al., 2001). Such indirect mechanisms of mast cell activation contribute to the UVBinduced systemic immunosuppression of acquired

¹Division of Human Immunology, Centre for Cancer Biology, Adelaide 5000, South Australia, Australia

²Schools of Molecular and Biomedical Sciences or Medicine, University of Adelaide, Adelaide 5000, South Australia, Australia

³Department of Pathology, Stanford University School of Medicine, Stanford, CA 94305

S.J. Galli and M.A. Grimbaldeston contributed equally to this paper.

²⁰¹⁰ Biggs et al. This article is distributed under the terms of an Attribution–Noncommercial–Share Alike–No Mirror Sites license for the first six months after the publication date (see http://www.rupress.org/terms). After six months it is available under a Creative Commons License (Attribution–Noncommercial–Share Alike 3.0 Unported license, as described at http://creativecommons.org/licenses/by-nc-sa/3.0/).

immune responses in mice subjected to a single acute dose (12 kJ/m²) of UVB irradiation (Hart et al., 1998, 2002). However, it is not clear how mast cells are activated when the skin is exposed to multiple cycles of UVB irradiation.

We investigated whether vitamin D_3 (or cholecalciferol), which has important effects in immunity (van Etten and Mathieu, 2005; Moro et al., 2008), might influence mast cell function during chronic low-dose UVB irradiation. Vitamin D_3 is synthesized in the epidermis upon UVB-induced photochemical conversion of 7-dehydrocholesterol to previtamin D_3 , which then undergoes spontaneous thermal isomerization to vitamin D_3 (Lehmann, 2005; Moro et al., 2008). Vitamin D_3 is converted into its biologically active metabolite, $1\alpha,25$ -dihydroxyvitamin D_3 ($1\alpha,25[OH]_2D_3$) via the 25-hydroxylation of vitamin D_3 by the cytochrome P450 proteins CYP2DII, CYP2D25, CYP3A4, or CYP2R1, followed by the hydroxylation of 25(OH) D_3 to $1\alpha,25(OH)_2D_3$ by CYP27B1 (Lehmann, 2005; Bouillon et al., 2008; Moro et al., 2008).

Recently, we reported evidence that mast cell production of the antiinflammatory cytokine IL-10 can limit the inflammation and tissue damage associated with chronic low-dose UVB irradiation of mouse skin (Grimbaldeston et al., 2007). UVB irradiation can increase production of vitamin D_3 , and mouse mast cells can express receptors for vitamin D_3 (i.e., vitamin D receptor [VDR]; Baroni et al., 2007). We therefore investigated whether $1\alpha,25(OH)_2D_3$ can activate mast cells to produce IL-10 and to what extent effects mediated via mast cell VDRs contribute to the mast cell's ability to curtail the skin pathology associated with chronic low-dose UVB irradiation.

RESULTS AND DISCUSSION

Vitamin D₃ activates mast cells to produce IL-10 without inducing degranulation

 $1\alpha,25(OH)_2D_3$ functions primarily by binding to its nuclear receptor, VDR, which recruits its preferred dimerization partner, the retinoid X receptor, to form a heterodimer that acts as a ligand-dependent transcription factor by binding to vitamin D response elements in the promoter regions of target genes (Kato et al., 2007; Bouillon et al., 2008). Many immune cells express VDRs, and $1\alpha,25(OH)_2D_3$ can elicit inhibitory effects in macrophages and dendritic cells (for review see van Etten and Mathieu, 2005), direct naive CD4⁺ T cells toward a Th2–IL–10–producing phenotype (Boonstra et al., 2001), and enhance the suppressive activity of CD4⁺CD25⁺ T cells (Gorman et al., 2007).

We found that C57BL/6J (B6) mouse BM-derived cultured mast cells (BMCMCs; i.e., B6- $VDR^{+/+}$ BMCMCs), like BALB/c BMCMCs (Baroni et al., 2007), expressed VDRs (Fig. 1 A) and, unlike B6- $VDR^{-/-}$ BMCMCs, exhibited increased levels of IL-10 mRNA 6 h after $1\alpha,25(OH)_2D_3$ stimulation (Fig. S1 A). Exposure to $1\alpha,25(OH)_2D_3$ for 24 h in vitro induced B6- $VDR^{+/+}$ BMCMCs to secrete IL-10 (Fig. 1 B), whereas for B6- $VDR^{-/-}$ BMCMCs levels of IL-10 were below the limit of detection (Fig. S1 B). Thus, mouse mast cells require functional VDRs to synthesize and release

IL-10 in response to $1\alpha,25(OH)_2D_3$. $1\alpha,25(OH)_2D_3$ stimulated the de novo synthesis and release of IL-10 by mast cells without inducing concomitant degranulation (Fig. S1 C). Thus, although both WT and $VDR^{-/-}$ BMCMCs degranulated (Fig. S2 A) and released IL-6 and TNF (Fig. S2, B and C) upon stimulation with IgE and specific antigen, BMCMCs did not degranulate in response to $1\alpha,25(OH)_2D_3$ (Fig. S1 C).

Absence of mast cell VDR exacerbates UVB-induced skin pathology

The finding that 1α,25(OH)₂D₃ induced BMCMCs to produce IL-10 in vitro raised the possibility that biologically active vitamin D₃ is the link between chronic low-dose UVB irradiation and mast cell IL-10 production (Grimbaldeston et al., 2007). To test this hypothesis, we exposed the ears of WT WBB6F₁-Kit^{+/+} (Kit^{+/+}) mice, mast cell-deficient WBB6F₁-KitW/W-v (KitW/W-v) mice, and KitW/W-v mice which had been engrafted with BMCMCs from WT (i.e., B6-VDR+/+) mice (WT BMCMC→Kit^{W/W-v} mice) or from B6-VDR-deficient mice ($VDR^{-/-}$ BMCMC $\rightarrow Kit^{W/W-v}$ mice) to one minimal erythema dose of UVB every 2 d for 15 exposures (total cumulative dose, 30 kJ/m² UVB). This UVB irradiation regimen resulted in scabbing of the ears, indicative of full-thickness epidermal necrosis and ulceration (Grimbaldeston et al., 2007), in 7/9 $Kit^{W/W-v}$ mice and 6/12 $VDR^{-/-}$ BMCMC $\rightarrow Kit^{W/W-v}$ mice, but in none of 11 WT mice or 9 WT BMCMC→ KitW/W-v mice (Table I). Moreover, compared with WT or WT BMCMC $\rightarrow Kit^{W/W-v}$ mice, mast cell-deficient $Kit^{W/W-v}$ mice and VDR^{-/-} BMCMC→Kit^{W/W-v} mice exhibited significantly greater increases in ear thickness after UVB irradiation (Fig. 2 A), with such differences being evident on day 8, just before the fifth UVB exposure, and continuing throughout the remainder of the UVB irradiation regimen.

After completion of the UVB irradiation regimen, mast cell–deficient *Kit*^{W/W-v} mice and *VDR*^{−/−} BMCMC→*Kit*^{W/W-v} mice exhibited more substantial skin pathology by histology

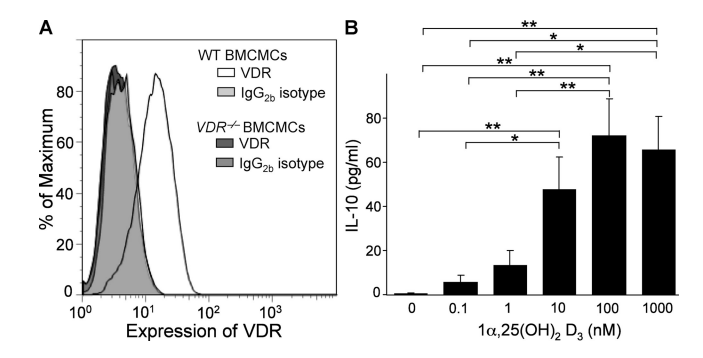


Figure 1. $1\alpha_2$ 5(OH)₂D₃-induced IL-10 production by BMCMCs. (A) FACS analysis of WT (B6) BMCMCs and $VDR^{-/-}$ BMCMCs for VDR expression. (B) IL-10 in supernatants of 5-wk-old (B6J) BMCMCs cultured for 24 h with 0.1–1,000 nM $1\alpha_2$ 5(OH)₂D₃. Data (n=5 per group) are of mean values obtained in five different experiments (all measurements for each experiment were performed in duplicate). *, P < 0.05 or **, P < 0.01 for the indicated comparisons. See Fig. S1 B for data using VDR^{-/-} BMCMCs.

Table I. Mast cell VDR expression is required for optimal limitation of full thickness epidermal necrosis associated with chronic low-dose UVB irradiation

UVB-treated mice	Mice with full thickness epidermal necrosis/total treated
WBB6F ₁ -Kit ^{+/+}	0 / 11
WBB6F ₁ -Kit ^{W/W-v}	7 / 9*
WT BMCMCs→Kit ^{W/W-v}	0 / 9
<i>VDR</i> ^{-/-} BMCMCs→ <i>Kit</i> ^{W/W-v}	6 / 12*

The data depict the numbers of mice whose ears exhibited scabbing (indicative of full thickness epidermal necrosis) and, in some cases, ulcers. Ears were assessed by clinical observation and/or histology during or at the end of the period of UVB exposure. *, P < 0.05 versus WT ($Kit^{+/+}$) mice or WT BMCMC-engrafted $Kit^{N/N--}$ (WT BMCMCs— $Kit^{N/N--}$); data summarize the results of the three independent experiments we performed (n = 3-4 mice/group per experiment), each of which gave similar results.

than did either of the other groups, including extensive dermal leukocyte infiltration, edema, and/or expansion of the dermis (Fig. 3, B, E, H, and K). The differences between the two groups of BMCMC-engrafted mice were not caused by disparities in the extent of mast cell engraftment, as similar numbers of ear pinna mast cells were present in the two groups (Fig. 2 B and Fig. 3, I and L).

As expected, the highly pigmented (black) WT mice had the smallest responses to UVB irradiation (Fig. 3, B and C). The capacity of UVB exposure to induce increased melanin pigmentation can further enhance the ability of the skin of WT mice to resist deleterious effects of UVB (Yamazaki et al., 2004; Melnikova and Ananthaswamy, 2005). By contrast, the white $Kit^{W/W-v}$ mice essentially lack skin melanocytes, as well as mast cells. Therefore, it is essential to compare the UVB-induced responses in the ears of mast cell–deficient $Kit^{W/W-v}$ mice with those in WT BMCMC $\rightarrow Kit^{W/W-v}$ mice

or $VDR^{-/-}$ BMCMC $\rightarrow Kit^{W/W-v}$ mice, as this enables assessment of mast cell contributions in the absence of confounding effects of skin pigmentation.

Epidermal thickening in response to UVB exposure also can enhance the resistance of the skin to some of the harmful effects of UV irradiation (Kligman, 1996). Moreover, functional VDRs may be required to mount an effective defense against excessive UV-induced damage (Ellison et al., 2008). Although all three groups of UVB-treated white $Kit^{W/W-v}$ mice (including the two BMCMC-engrafted groups) exhibited significantly more epidermal thickening than the UVB-treated WT mice, the presence of either WT or $VDR^{-/-}$ mast cells resulted in significantly reduced UVB-induced epidermal thickening than was observed in mast cell–deficient $Kit^{W/W-v}$ mice, with WT mast cells exhibiting a larger protective effect than $VDR^{-/-}$ mast cells (Fig. S3).

Mast cell VDRs are required for optimal curtailment of UVB-induced inflammation

The UVB-induced ear swelling responses (Fig. 2 A) and pathology (Fig. 3 K) of $VDR^{-/-}$ BMCMC $\rightarrow Kit^{W/W-v}$ mice resembled those observed in IL- $10^{-/-}$ BMCMC $\rightarrow Kit^{W/W-v}$ mice. We confirmed our finding (Grimbaldeston et al., 2007) that the ear skin of UVB-treated mast cell–deficient $Kit^{W/W-v}$ mice, compared with the identically treated skin of WT BMCMC $\rightarrow Kit^{W/W-v}$ mice or WT mice, contained significantly higher numbers of every population of granulocytes, macrophages, or CD4⁺ T cells analyzed (Fig. 4). Adult WBB6F₁– $Kit^{W/W-v}$ mice have reduced numbers of neutrophils in the BM, blood, and spleen (Chervenick and Boggs, 1969; Nigrovic et al., 2008; Piliponsky et al., 2010). Despite the possibility that this neutrophil deficiency might influence inflammatory responses in $Kit^{W/W-v}$ mice, all three groups of $Kit^{W/W-v}$ mice tested (i.e., those with or without

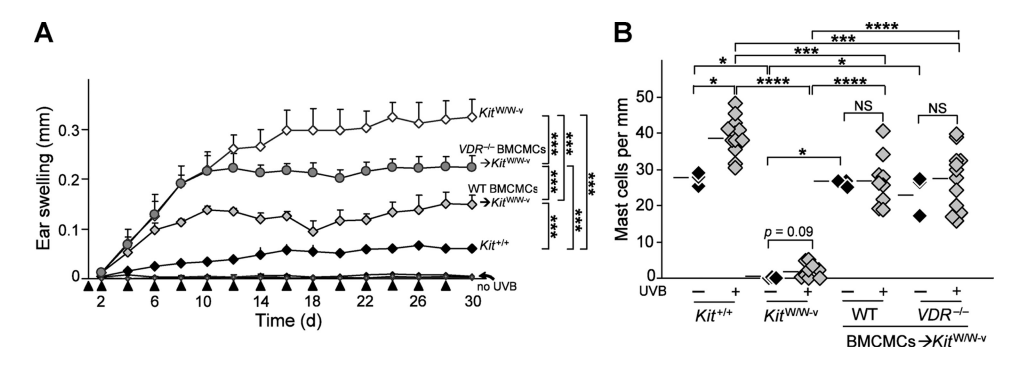


Figure 2. Mast cell VDR expression helps to limit tissue swelling associated with chronic low-dose UVB irradiation. (A) Ear swelling after 15 exposures to 2 kJ/m² of UVB (each arrowhead indicates a single exposure) in WT WBB6F₁- $Kit^{\text{W/W-v}}$ mice (black diamond, $Kit^{\text{W/W-v}}$; n = 11), mast cell-deficient WBB6F₁- $Kit^{\text{W/W-v}}$ mice (open diamond, $Kit^{\text{W/W-v}}$; n = 9), and WBB6F₁- $Kit^{\text{W/W-v}}$ mice engrafted in the ear pinnae with WT C57BL/6- $VDR^{\text{r/+}}$ BMCMCs (light gray diamond, WT BMCMC— $Kit^{\text{W/W-v}}$, n = 9) or $VDR^{-/-}$ BMCMCs (dark gray circle, $VDR^{-/-}$ BMCMC— $Kit^{\text{W/W-v}}$; n = 12). ***, P < 0.0001 for the indicated comparisons between groups of UVB-irradiated mice. Data (n = 9-12 per group) are from the three independent experiments performed (each with three to four mice per group), each of which gave similar results. Ear swelling measurements in ears not irradiated with UVB ("no UVB") are highly overlapping for the four groups of mice; for each group, responses in UVB-irradiated ears were significantly different from those in the non-UVB-irradiated ears at P < 0.0001. (B) Numbers of dermal mast cells in ear pinnae after 15 exposures to 2 kJ/m² of UVB. *, P < 0.05; **, P < 0.001; or ****, P < 0.001; or ****, P < 0.0001, for the indicated comparisons. Data (3–12 mice per group) are from the three experiments performed, each of which gave similar results; each experiment analyzed one ear from a mouse not treated with UVB (– UVB) and single ears from three to four UVB-treated (+ UVB) mice.

adoptively-transferred mast cells) had significantly higher numbers of granulocytes in the UVB-treated ears than the identically-treated WT mice, with mast cell–deficient $Kit^{W/W-v}$ mice exhibiting the highest level of infiltrating granulocytes (Fig. 4 A and B). Also, numbers of $Gr-1^{hi}$ granulocytes, as well as $CD4^+$ and $CD4^+CD25^+CD62L^-$ T cells, in UVB-exposed ear skin of $VDR^{-/-}$ BMCMC $\to Kit^{W/W-v}$ mice were significantly lower than in mast cell–deficient $Kit^{W/W-v}$ mice but higher than in WT BMCMC $\to Kit^{W/W-v}$ mice (Fig. 4, B and D). Thus, although adoptively transferred $VDR^{-/-}$ mast cells limited numbers of leukocytes in the UVB-treated skin of WBB6F₁- $Kit^{W/W-v}$ mice, they were not as effective as WT mast cells.

Notably, the highest levels of CD4⁺CD25⁺FoxP3⁺ T cells (a subset of regulatory T cells that has been implicated in a mast cell–dependent pathway required for normal expression of peripheral tolerance to skin allografts (Lu et al., 2006)) were observed in the groups of mice that developed the most severe inflammation: WBB6F₁– $Kit^{W/W-v}$ mice and, to a lesser extent, $VDR^{-/-}$ BMCMC $\rightarrow Kit^{W/W-v}$ mice (Fig. 4 D). Much lower levels of CD4⁺CD25⁺FoxP3⁺ T cells, which were statistically indistinguishable from those observed in the UVB-irradiated skin of WT BMCMC $\rightarrow Kit^{W/W-v}$ mice (Fig. 4 D). This finding does not exclude the possibility that mast cells can enhance resistance to adverse effects of chronic UVB irradiation in part by effects on

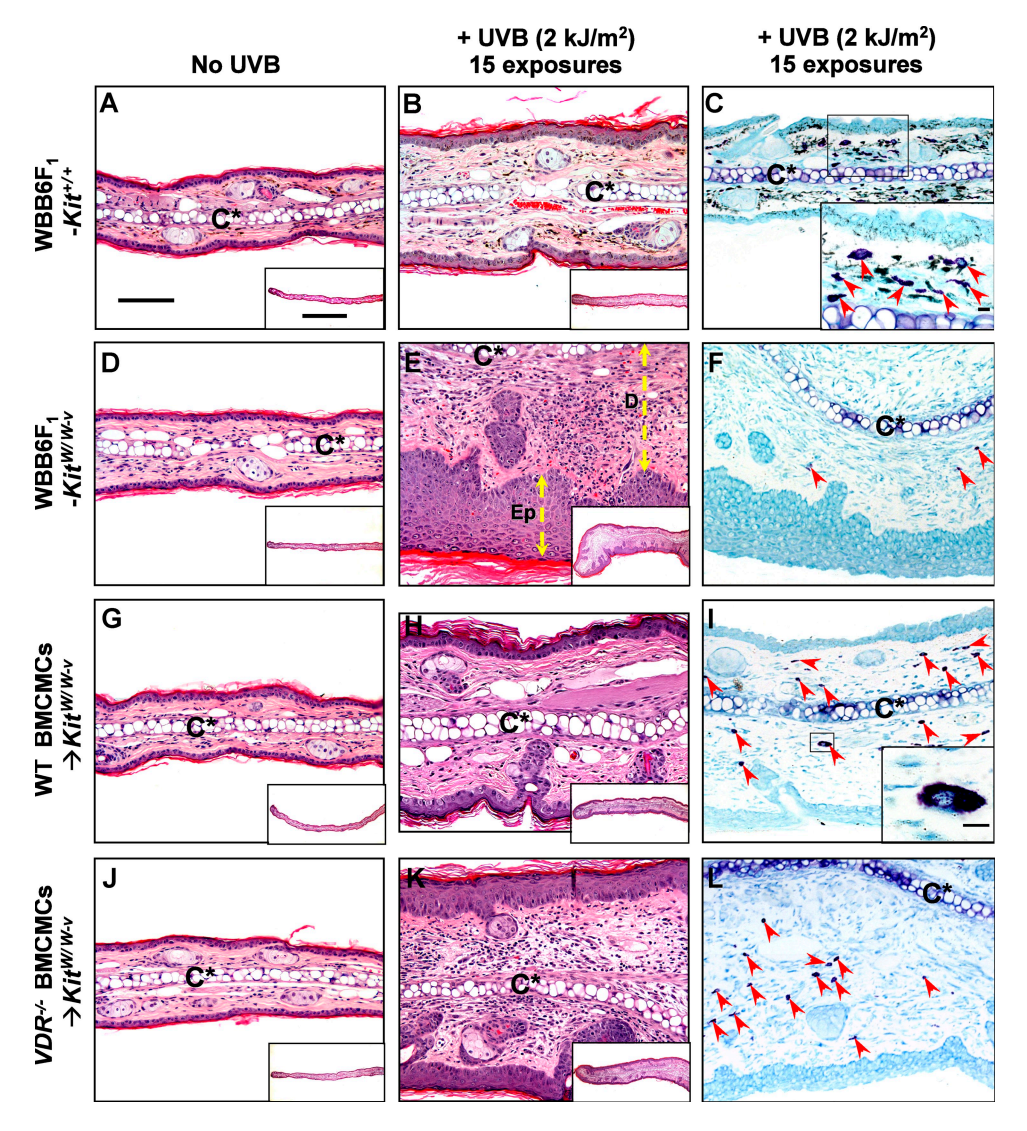


Figure 3. Mast cells and mast cell VDR expression are required to limit pathology induced by chronic low-dose UVB irradiation of ear skin. Cross sections of ears obtained from WBB6F₁- $Kit^{+/l}$ (WT) mice (A–C), WBB6F₁- $Kit^{+/l/l}$ (WT) mice (D–F), WT BMCMC $\rightarrow Kit^{+/l/l}$ mice (G–I), or $VDR^{-/-}$ BMCMC $\rightarrow Kit^{+/l/l}$ mice (J–L) at 24 h after the final exposure to 2 kJ/m² UVB (15 exposures, 2 d apart; B, C, E, F, H, I, K, and L); sections stained with H&EE (A, B, D, E, G, H, J, and K), or Toluidine blue (C, F, I, and L). Mice that did not receive UVB irradiation were also killed for analysis of skin histology at the end of the experiment (A, D, G, and J). C*, cartilage. Double-headed arrows indicate thickness of dermis (D) or epidermis (Ep). Red arrowheads indicate mast cells (C, F, I, and L). Bars: 100 µm (inset in A; for A–L); 1,000 µm (A; for insets in A, B, D, E, G, H, J, and L); 10 µm (C and I insets). Results are representative of those obtained in the three different experiments performed, each with three to four mice analyzed per group.

CD4+CD25+FoxP3+ T cells, but our results do show that large numbers of such cells can appear in UVB-irradiated skin that is essentially devoid of mast cells. These results are consistent with the possibility that, in settings in which there is little or no mast cell–dependent suppression of inflammation, there can be a compensatory increase in the deployment of other mechanisms that can reduce tissue damage, including those mediated by regulatory T cells.

Our findings strongly support the conclusion that optimal mast cell–dependent suppression of the inflammation and tissue pathology associated with chronic UVB irradiation of the skin of WBB6F₁–*Kit*^{W/W-v} mice requires that mast cells express VDR. However, other mechanisms of mast cell activation probably also contribute to their anti-inflammatory effects in this setting, as some features of the pathology induced by chronic UVB irradiation were reduced in WBB6F₁–*Kit*^{W/W-v} mice that had been engrafted with *VDR*^{-/-} mast cells. Based on prior work with various models of UVB irradiation of mouse skin, such mechanisms of dermal mast cell activation may include keratinocyte–derived nerve growth factor (Hart

et al., 2002; Townley et al., 2002), neuropeptides derived from sensory C fibers (Hart et al., 2002), and locally produced endothelin-1 (Metz et al., 2006). However, it remains to be determined whether these mechanisms of mast cell activation occur during our model of chronic UVB irradiation.

Loss of mast cell VDRs alters the cytokine profile in UVB-irradiated skin

We assessed cutaneous levels of IL-10, IL-4, IL-6, and TNF 24 h after either the 4th or 15th exposure to UVB irradiation (Fig. 5, A–D). We confirmed our prior finding (Grimbaldeston et al., 2007) that after 15 UVB exposures skin levels of IL-10 were higher in WT $Kit^{+/+}$ mice and in WT BMCMC $\rightarrow Kit^{W/W-v}$ mice than in mast cell–deficient $Kit^{W/W-v}$ mice, and we also found that skin IL-10 levels in $VDR^{-/-}$ BMCMC $\rightarrow Kit^{W/W-v}$ mice were not significantly different from those in mast cell–deficient $Kit^{W/W-v}$ mice (Fig. 5 A). The highest levels of IL-10 were observed in WT BMCMC $\rightarrow Kit^{W/W-v}$ mice after four UVB exposures, coinciding with the start of lower ear swelling responses in these mice

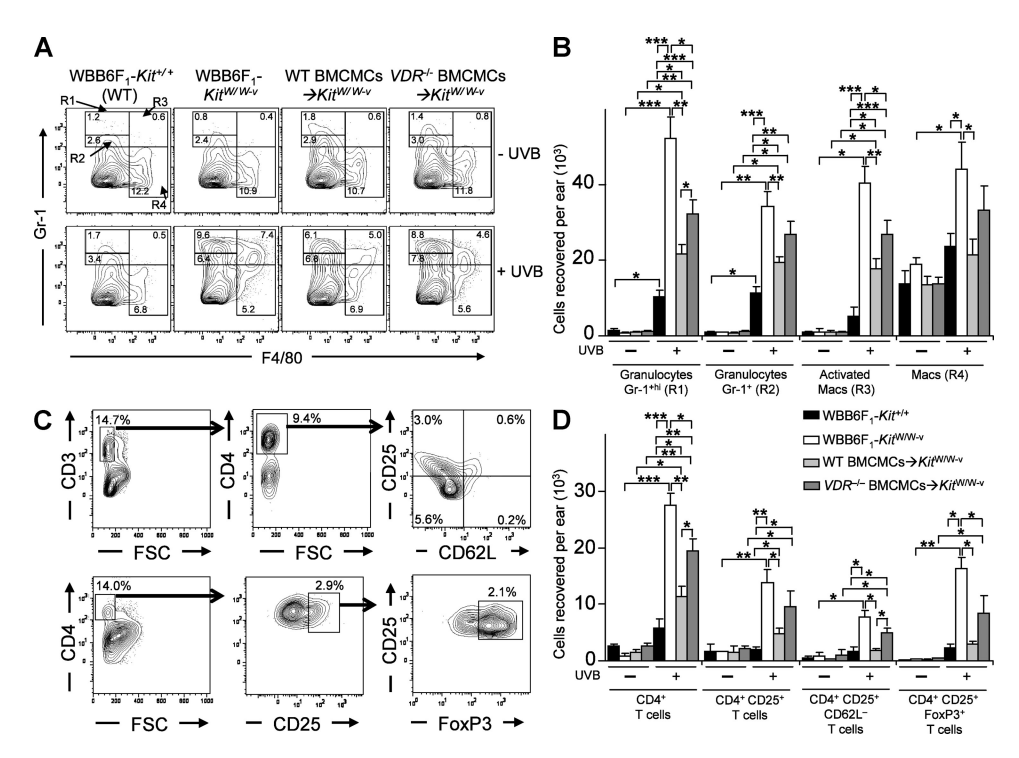


Figure 4. Mast cell VDR expression helps to limit leukocyte numbers in ear skin exposed to chronic low-dose UVB irradiation. Flow cytometric analysis of granulocytes and macrophages (A and B) and CD4+ and CD4+CD25+ T cells (C and D) 24 h after the last of 15 exposures to 2 kJ/m² UVB irradiation (+ UVB) or at control sites not treated with UVB irradiation (- UVB) in ear skin of WBB6F₁- $Kit^{+/+}$ (WT) mice, mast cell-deficient WBB6F₁- $Kit^{+/+}$ ($Kit^{+/-+}$) mice, WT BMCMC $\rightarrow Kit^{+/--}$ BMCMC $\rightarrow Kit^{+/--}$ BMCMC $\rightarrow Kit^{+/--}$ mice. Percentage values in A and C refer to percentage of total viable cells present in the depicted section of the plot. (A) Representative FACS plots of granulocytes and macrophages in ears derived from individual mice. (B) Granulocytes (gated population R1, Gr-1^{hi}; R2, Gr-1⁺) and macrophages (macs; R3 ["activated macrophages"], F4/80+ Gr-1^{hi}; R4, F4/80+) recovered per ear. (C) Representative FACS plots of T cell populations in ears derived from individual mice, where live populations of CD3+ T cells were first gated and then CD4+CD25+CD62L- T cells were selected, and where 4% paraformaldehyde-fixed CD4+ T cells were gated, and then CD25+ FoxP3+ T cells were selected. Percentages of gated T cell populations indicated are the percentage of the total cell population in that ear. (D) CD4+ T cell populations recovered per ear based on flow cytometric analysis of fixed cells (for CD4+CD25+FoxP3+ T cells) or live cells (the other three groups). (B and D) Data (n = 6-12 per group) are of mean values from 3 different experiments, each of which gave similar results, in which individual ears of three to four mice per group were analyzed in each experiment. *, P < 0.05; **, P < 0.01; ****, P < 0.001 for the indicated comparisons.

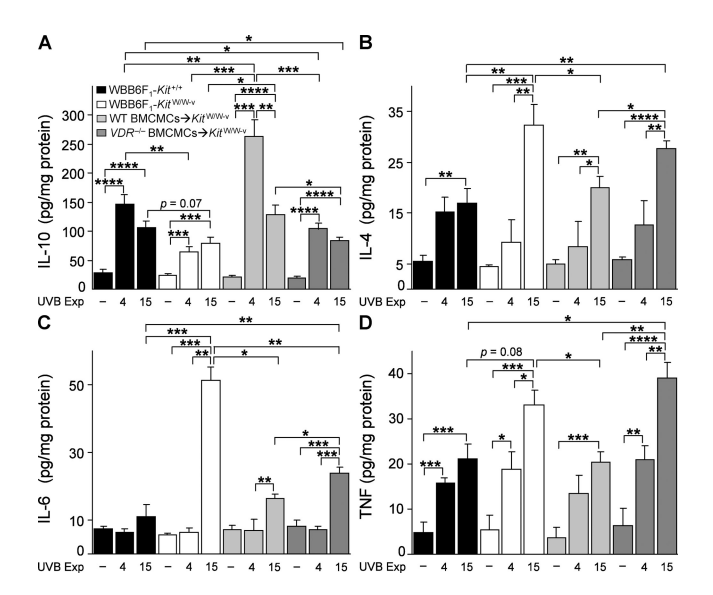


Figure 5. Ear skin cytokine levels 24 h after 4 or 15 UVB exposures. Levels of IL-10 (A), IL-4 (B), IL-6 (C), and TNF (D) in lysates of control ears not treated with UVB irradiation (– UVB) or ears treated with 4 or 15 exposures to 2 kJ/m² UVB irradiation in WBB6F₁– $Kit^{+/+}$ (WT) mice, mast cell–deficient WBB6F₁– $Kit^{+/-}$ ($Kit^{+/-}$) mice, WT BMCMC $\rightarrow Kit^{+/-}$ mice, and $VDR^{-/-}$ BMCMC $\rightarrow Kit^{+/-}$ mice. Data (n=6–8 per group) are from the two experiments performed, each of which gave similar results, in which three to four mice/group were tested per experiment. *, P < 0.05; ***, P < 0.01; ****, P < 0.001; *****, P < 0.0001 for the indicated comparisons.

versus $Kit^{\text{W/W-v}}$ or $VDR^{-/-}$ BMCMC $\rightarrow Kit^{\text{W/W-v}}$ mice (Fig. 2 A). However, levels of skin IL-10 in all groups of UVB-treated mice exceeded those in the corresponding control groups. In addition to mast cells, other potential sources of UVB-induced IL-10 in this model include keratinocytes, endothelial cells, macrophages and dendritic cells (Nishigori et al., 1996; Wolf et al., 2000), as well as CD4⁺ T cells (particularly the CD4⁺CD25⁺ and FoxP3⁺ subsets (Beissert et al., 2006)). 1α ,25(OH)₂D₃ can stimulate Th2 development of CD4⁺ T cells, with increased production of IL-4, IL-5 and IL-10 (Boonstra et al., 2001); CD4⁺ T cells thus also represent one potential source of the higher amounts of IL-4 protein observed in $Kit^{\text{W/W-v}}$ mice and $VDR^{-/-}$ BMCMC $\rightarrow Kit^{\text{W/W-v}}$ mice compared with the other two groups after 15 UVB exposures (Fig. 5 B).

IL-6 production by keratinocytes is thought to contribute to UVB-induced cutaneous inflammation (Kirnbauer et al., 1991). $Kit^{W/W-v}$ mice had the highest levels of IL-6 after 15 UVB exposures (Fig. 5 C) and exhibited the most extensive skin pathology (Fig. 2 A; Fig. 3; and Fig. 4, B and D). IL-6 can induce keratinocyte proliferation, suggesting that IL-6 also may contribute to the UVB-induced epidermal hyperplasia in $Kit^{W/W-v}$ mice (Fig. 3 E and Fig. S3). Accordingly, UVB-treated $VDR^{-/-}$ BMCMC $\to Kit^{W/W-v}$ mice exhibited levels of skin IL-6 and epidermal thickening that were intermediate between those of $Kit^{W/W-v}$ mice and WT BMCMC $\to Kit^{W/W-v}$ mice (Fig. 3, D–L; Fig. 5 C; and Fig. S3).

UVB-irradiated skin of KitW/W-v mice and VDR-/-BMCMC→Kit^{W/W-v} mice also exhibited higher levels of TNF than those in UVB-treated skin of WT mice or WT BMCMC→Kit^{W/W-v} mice (Fig. 5 D). TNF may have a proinflammatory role (Galli et al., 2008) in this setting, but TNF has pleiotropic activities and has been implicated as a potential immunosuppressive cytokine in some models of UVB irradiation (Alard et al., 1999). Although the factors that regulate the levels and function of cytokines at sites of UVB irradiation are complex, our results indicate that, in our model of chronic UVB irradiation, dermal mast cells have effects that can increase levels of IL-10 and decrease levels of IL-4, IL-6, and TNF, at least in the skin of KitW/W-v mice. Moreover, to perform such roles most effectively (particularly, to increase levels of IL-10 [Fig. 5 A] or to decrease levels of TNF [Fig. 5 D]), dermal mast cells must express VDR.

We also analyzed levels of $1\alpha,25(OH)_2D_3$ in the skin after five UVB exposures, corresponding to the time when mast cell–deficient $Kit^{W/W-v}$ mice and $VDR^{-/-}$ BMCMC $\rightarrow Kit^{W/W-v}$ mice exhibited significantly greater increases in ear thickness in response to UVB irradiation than did WT or WT BMCMC $\rightarrow Kit^{W/W-v}$ mice (Fig. 2 A). In all four groups of mice, UVB irradiation resulted in similar, and statistically significant, increases in levels of $1\alpha,25(OH)_2D_3$ in the skin (Fig. S4).

In conclusion, we found that mouse mast cells exposed to biologically active 1α,25(OH)₂D₃ can produce IL-10 in vitro, and that the ability of mast cells to limit the skin inflammation and injury, and to enhance cutaneous levels of IL-10, associated with chronic low-dose UVB irradiation in vivo depends, at least in part, on mast cell expression of functional VDRs. Our data thus suggest that biologically active $1\alpha,25(OH)_2D_3$, whose levels are increased after UVB irradiation of the skin, can contribute importantly both to the activation of dermal mast cells and to the regulation of skin pathology associated with extensive UVB exposure. The nature of the mast cell's responses to UVB irradiation may depend on the intensity and duration of the UVB exposure, and may vary in different species. However, our results in WBB6F1-KitW/W-v mice define chronic exposure to UVB irradiation as a setting in which responsiveness to $1\alpha,25(OH)_2D_3$ via mast cell–associated VDR can promote antiinflammatory effects of mast cells which in turn can substantially limit cutaneous pathology. Our findings also raise the possibility that inducing antiinflammatory activities of mast cells by exposure to 1α,25(OH)₂D₃ might represent a novel approach for reducing inflammation and tissue damage in this and perhaps other settings.

MATERIALS AND METHODS

Mice. Female C57BL/6J (B6) mice, *VDR*-targeted VDR-deficient B6.129S4-*Vdr*^{tm1Mbd}/J mice backcrossed to C57BL/6 mice for greater than eight generations (*VDR*^{-/-} mice), and c-kit mutant genetically mast cell-deficient (WB/ReJ-*Kit*^{W/-} x C57BL/6J-*Kit*^{W/-})+F₁-*Kit*^{W/-} (WBB6F₁-*Kit*^{W/-}) (Kit^{W/W-t}) mice and the congenic normal WBB6F₁-*Kit*+++ (Kit+++) mice, were obtained from The Jackson Laboratory and bred in house, either at Stanford University or at the Centre for Cancer Biology (Adelaide, Australia). All mice were provided ad libitum commercial mouse chow containing Vitamin D₃ (cholecalciferol) at >2,000 IU/kg (Specialty Feeds). Adult *Kit*^{W/W-t}

mice have a profound deficiency of mast cells, including <1.0% the WT level of mast cells in the dermis (Galli et al., 2005, 2008). All in vivo experiments were performed with age-matched female mice of at least 10 wk of age. Experiments were performed in compliance with the ethical guidelines of the National Health and Medical Research Council of Australia or with the "Guide for the Care and Use of Laboratory Animals" prepared by the Institute of Laboratory Animal Resources, National Research Council, and published by the National Academy Press and with approval from the Institute of Medical and Veterinary Science Animal Ethics Committee (Australia) and the Stanford Institutional Animal Care and Use Committee.

Preparation and adoptive transfer of BMCMCs into mast cell-deficient mice. As previously described (Grimbaldeston et al., 2007), BMCMCs were obtained by culturing BM cells from femurs of female mice in 20% WEHI-3 conditioned medium (containing IL-3) for 4–6 wk, at which time >95% of the cells were identified as mast cells by May Grunwald-Giemsa staining and by flow cytometric analysis (c-Kit+ FcεRI+). For mast cell engraftment studies, BMCMCs derived from WT C57BL/6-VDR+/+ (WT BMCMCs) or C57BL/6-VDR-/- (VDR-/- BMCMCs) mice were transferred by intradermal injection (i.d.; 2 injections into each ear of 106 cells in 25 μl DMEM/each injection) into 4–6 wk old *KitWW-ν* mice. Chronic low-dose UVB experiments were initiated 6–8 wk after i.d. transfer of BMCMCs.

UV irradiation. For UV irradiation of mice, a bank of 6 Philips FS40T12 lamps (Ultraviolet Resources International) emitting a broad 270-380-nm band of UV, with peak emission at 310 nm comprising ~65% of the energy emitted, was used to irradiate mice in individual compartments of perspex cages. The intensity and spectral output of the UVB lamps were measured using a UVX spectrophotometer with a UVX-31 sensor (UV products). A new sheet of clear PVC plastic film (0.23 mm thick) was taped to the top of each perspex cage before irradiation to screen wavelengths <290 nm. Sunlamps were held 15 cm above the cages. 10-14-wk-old mice were conscious and had full range of movement during irradiation. For chronic exposures the entire mouse (including both ears) was irradiated with a dose of 2 kJ/m² UVB (i.e., equivalent to 1 minimal erythema dose as previously determined for albino mast cell-deficient WBB6F₁-Kit^{W/W-v} mice; Grimbaldeston et al., 2007), every 2 d for a total of 4 or 15 exposures (total cumulative dose = 8 kJ/m² or 30 kJ/m² UVB, respectively). Ear thicknesses were measured using a micrometer (Ozaki MFG. CO., LTD.) before each UVB irradiation. Mice were killed by CO2 inhalation 24 h after the final UVB exposure and samples of ear were taken for histology, FACS analysis, and IL-10, IL-4, IL-6, and TNF protein measurements.

Histology and quantification of mast cell numbers and epidermal thickness. Mice were killed by CO2 inhalation and samples of ear pinna were fixed in 10% buffered formalin, embedded in paraffin (with care to ensure a cross-sectional orientation), and 4-µm sections were cut. Ear sections were stained with hematoxylin and eosin (H&E) stain, or with 0.1% Toluidine blue, pH 1.0, for the detection of mast cells (cytoplasmic granules appear purple). Ear pinna mast cells were counted in 6-9 consecutive fixed fields of 870 µm width using a 10× microscope objective (final magnification = 100×), and mast cell numbers were expressed per horizontal ear cartilage field length (millimeter), using computer-generated image analysis (NIH Image J software, version 1.29×). The entire length of a strip of skin extending from the base to the tip of the ear pinna (~5.22-7.83 mm) was quantified. After i.d. engraftment of BMCMCs, KitW/W-v mice exhibited mast cells from the base to the tip of the ear pinnae, in an anatomical distribution similar to that of the native mast cell populations in the corresponding WT mice. For quantification of epidermal thickness, images of 12-30 consecutive microscopic fields (435 µm width) of H&E-stained cross sections of ear skin from each mouse (n = 6-8/group), performed perpendicular to the epidermis, were captured using a 20× microscope objective (200× final magnification). For each image, eight randomly selected measurements of the distance between the stratum corneum and the bottom of the basal layer

were recorded and epidermal thickness is expressed as mean + SEM per mm of ear cartilage.

Measurement of 1α,25(OH)₂D₃ in ear skin lysates. Ear skin samples were obtained from mice 24 h after the last of 5 UVB exposures delivered 2 d apart (each of the 5 exposures was to 2 kJ/m² UVB) or from control (no UVB treatment) mice, and levels of 1α,25(OH)₂D₃ were measured using a radioimmunoassay kit according to the manufacturer's instructions (Immunodiagnostic Systems Ltd). For preparation of mouse ear skin lysates, each ear was weighed, split in half along the cartilage and then finely cut up on an ice cold surface. Tissue was then snap frozen in liquid nitrogen and placed on ice, and then 250 µl of a chloroform-methanol (1:2 vol/vol) extraction mixture was added and samples were further disrupted by sonication. Ear skin lysates were stored overnight at -80°C, and then centrifuged at 17,000 g for 10 min at 4°C. The supernatant was collected and the chloroform-methanol extraction solution evaporated under continuous airflow in a chamber until only 50 µl remained. After the addition of 150 µl of 1 x PBS, ear skin lysates were then ready for analysis of $1\alpha,25(OH)_2D_3$ using the RIA kit. 200 μl of ear skin lysate from each mouse was analyzed. Each step in the preparation of the ear skin lysates was performed shielded from light. The data obtained were expressed as picomole/milligram of tissue.

Measurement of cytokines in ear skin lysates. Ear skin lysates were prepared as previously described (Grimbaldeston et al., 2007) and IL-10, IL-4, IL-6, and TNF protein levels in the supernatants were measured by ELISA (IL-10 and IL-4 kits; eBioscience; IL-6 and TNF OptEIA kits; BD), according to the manufacturer's instructions, and data obtained from each group were expressed as mean + SEM picogram/milligram protein. The lower limits of detection were as follows: IL-10 = 30 pg/ml; IL-4 = 4 pg/ml; IL-6 = 15.6 pg/ml; TNF = 15.6 pg/ml. Total protein levels in the supernatants were measured by a Bio-Rad D_c protein assay, according to the manufacturer's instructions (Bio-Rad Laboratories).

BMCMC stimulation and cytokine measurement. At 5 wk of culture, BMCMCs (2 \times 10⁶ cells/ml) were stimulated with $1\alpha,25(OH)_2D_3$ (Sigma-Aldrich) at the various concentrations tested in DMEM (Sigma-Aldrich) containing WEHI-3-conditioned medium for 24 h and IL-10 protein levels in the supernatants were measured by ELISA. For stimulation of BMCMCs with IgE, 106 cells/ml were preloaded with IgE anti-DNP mAb (generated from ascites induced by the hybridoma H1-DNP-ε26, which produces an IgE mAb to DNP [provided by F.-T. Liu, University of California-Davis, California, and D.H. Katz, AVANIR Pharmaceuticals, Aliso Viejo, CA]) at a concentration of 2 µg/ml in medium containing WEHI-3-conditioned medium overnight at 37°C. The mast cells were then washed with DMEM supplemented with 0.1% BSA, centrifuged at 1,000 rpm (250 g) for 5 min at 4°C, plated at 106 cells/ml in 0.1% BSA DMEM, and stimulated for 6 h with 20 ng/ml of DNP-HSA-specific antigen (30-40 DNP conjugated to each molecule of HSA [DNP₃₀₋₄₀-HSA]; Sigma-Aldrich). Levels of IL-6, TNF, and IL-10 in the supernatants were measured using ELISA.

β-Hexosaminidase degranulation assay. Cells were washed with Tyrodes buffer (10 mM Hepes, 129 mM NaCl, 5 mM KCl, 1.4 mM CaCl₂, 1 mM MgCl₂, 8.4 mM glucose, and 0.1% BSA), centrifuged, resuspended in Tyrodes buffer, plated at a concentration of 2.25×10^6 cells/ml in each well of a 96-well v-bottom plate with increasing concentrations of 1α ,25(OH)₂D₃ (0.1–1,000 nM) and incubated at 37°C for 1 or 3 h. As a positive control, 50 ng/ml PMA/10 μM calcium ionophore A23187 (Sigma-Aldrich) was included for one treatment group. Cell supernatants were collected by centrifugation at 1,000 rpm (250 g) for 5 min, and the cell pellet was lysed using 0.5% Triton X–100 in Tyrodes buffer. Cell supernatants and pellet lysates were incubated with 4 mM p-nitrophenyl-N-acetyl-β-D-glucosaminidine (Sigma-Aldrich) in substrate buffer (155 mM Na₂HPO₄ and 88 mM citric acid, pH 4.5) for 1 h at 37°C. β-Hexosaminidase activity was detected by addition of 0.2 M glycine, pH 10.7, and absorbance at 405 nm was measured

on an enzyme-linked immunosorbent assay "reader." Percentage of degranulation was calculated by dividing the β -hexosaminidase activity in the cell supernatant by the total β -hexosaminidase activity detected (supernatant plus pellet). For measurement of degranulation induced by IgE anti-DNP + specific antigen, the protocol outlined above was performed with the exception that BMCMCs were preloaded with 2 $\mu g/ml$ of IgE anti-DNP mAb in DMEM containing WEHI-3–conditioned medium overnight, and stimulated with increasing concentrations of DNP-HSA in Tyrodes buffer for 1 h at 37°C.

Flow cytometric analysis and antibodies. After 4% paraformaldehyde fixation of BMCMCs for 15 min at room temperature, cells were incubated with rat anti-VDR antibody (Millipore) or isotype control rat IgG2b antibody in PBS containing 0.1% saponin for 30 min on ice. Cells were washed, incubated with anti-rat PE-conjugated antibody (Invitrogen) for 30 min on ice, and then analyzed on a FACSCalibur (BD) and using FlowJo Software (version 5.7.2; Tree Star, Inc.). For assessment of leukocyte populations in UVB-irradiated or naive ears, individual ears of each mouse in each treatment group were analyzed in a given experiment. As previously described (Grimbaldeston et al., 2007), ear skin was split parallel with the cartilage into two halves, cut into fine pieces and incubated in RPMI plus 0.5 mg/ml of Liberase CI (Roche) for 1 h at 37°C. A suspension of single cells was obtained by using a 70-µm nylon cell strainer to separate undigested tissue. Suspensions of single cells were incubated with anti-mouse CD16/CD32 mAb (eBioscience) on ice for 15 min. After FcR blocking, leukocytes were incubated on ice for 40 min with antibodies reactive with the following cell surface markers: anti-mouse CD3e (145-2C11, 2 µg/ml); CD4 (RM4-5, 2 μg/ml); CD8β (CT-CD8b,1 μg/ml); CD25 (PC61.5, 5 μg/ml); CD62L (MEL-14, 2 $\mu g/ml);$ F4/80 (BM8, 1 $\mu g/ml);$ and Gr-1 (Ly-6C RB6-8C5, $0.5 \,\mu g/ml$). All of these antibodies were obtained from eBioscience with the exception of the Gr-1 mAb, which was obtained from BD. Gates for subpopulations of cells were based on isotype control antibody staining (Rat IgG2b, Rat IgG2a), as well as single color staining of the cells to assess compensation and nonspecific fluorescence. 7-aminoactinomycin D (7-AAD) was used to detect dead cells. Only cells negative for 7-AAD were analyzed. To calculate the number of live cells of a particular type recovered per ear (determined by gating on 7-AAD-negative cells), the following calculation was applied for each population quantified: live cells recovered per ear in a particular subset of leukocytes = (percentage gated of the total cell population in that ear) \times (total number of cells recovered from that ear [counted using a hemacytometer after tissue digestion and single cell suspension]). For FoxP3 intracellular staining of CD4⁺ T cells, submaxillary lymph node cells or single cell suspensions of ear-derived cells were incubated with antibodies for surface markers (i.e., α-CD3, α-CD4, and α-CD25), fixed in 1% paraformaldehyde, and then incubated with anti-mouse FoxP3-PE according to the kit instructions (eBioscience).

RNA extraction and real-time PCR. Total RNA was extracted from BMCMCs (5 \times 10⁶ cells) using Trizol (Invitrogen), according to the manufacturer's instructions. For mRNA analysis, 2 µg of RNA was used for complementary DNA (cDNA) synthesis using the Omniscript reverse transcription kit (QIAGEN) and oligo (dT)₁₂₋₁₈ (Invitrogen). Quantitative real-time PCR was performed using a 1:4 dilution of cDNA with the QuantiTect SYBR Green PCR system (QIAGEN) on a Rotor-Gene 6000 PCR machine (Corbett Research). PCR assays were performed for 45 cycles (95°C for 15 s, 52°C for 20 s, and 72°C for 20 s). Relative expression levels of IL-10 mRNA were normalized to a β-actin control using the Rotor-Gene Series 6000 Software (Corbett Research). For assessment of $1\alpha,25(OH)_2D_3$ -induced IL-10 mRNA expression, total RNA and then cDNA was prepared from BMCMCs that were stimulated for 6 h with increasing concentrations of 1α,25(OH)₂D₃ (10-1,000 nM). The following oligonucleotide sequences were used: IL-10, forward 5'-GCCTTATCG-GAAATGATCCA-3', reverse 5'-TTCTCACCCAGGGAATTCAA-3'; and β-actin, forward 5'-TGGAATCCTGTGGCATCCATGAAAC-3', reverse 5'-TAAAACGCAGCTCAGTAACAGTCCG-3'.

Statistical analysis. Analysis of variance (ANOVA) for repeated measures was used to assess differences in ear swelling between groups of mice over the course of the chronic UVB regimen. For all of our pairwise comparisons of the data, before pairwise testing, a one-way ANOVA between groups was performed and pairwise analysis using the unpaired, two-tailed, Student's t test was only considered when the ANOVA analysis indicated statistical significance. For the occurrence of focal epidermal scabbing and necrosis, we employed the χ^2 test for comparisons between groups. P values >0.05 were considered statistically significant. Unless otherwise specified, all data are presented as mean + SEM.

Online supplemental material. Fig. S1 shows that $1\alpha,25(OH)_2D_3$ can increase IL-10 mRNA levels and induce release of IL-10 in WT BMCMCs, but not in *VDR*-deficient BMCMCs, but without inducing BMCMC degranulation. Fig. S2 shows that VDR-deficient and WT mast cells exhibit similar levels of IgE- and antigen-dependent degranulation and cytokine production. Fig. S3 shows the influence of mast cell VDR expression on the ability of mast cell populations to limit epidermal thickness associated with chronic low-dose UVB irradiation of ear skin. Fig. S4 shows that levels of $1\alpha,25(OH)_2D_3$ in ear skin are increased 24 h after the fifth exposure to UVB irradiation. Online supplemental material is available at http://www.jem.org/cgi/content/full/jem.20091725/DC1.

We thank Chen Liu for help with histology, Eon J. Rios for advice on FACS, Mindy Tsai for helpful discussions, F.-T. Liu and D. H. Katz for IgE anti-DNP mAb-producing mouse H1-DNP- ϵ 26 hybridoma cells, Thomas Sullivan for advice on statistical analyses, and Paul Anderson and Rebecca Sawyer (Hanson Institute) for help with tissue measurements of 1α ,25(OH)₂D₃.

This work was supported by an Australian National Health and Medical Research Council (NHMRC) Career Development Award Fellowship and NHMRC project grant (to M.A. Grimbaldeston), and United States Public Health Service grants Al23990, Al070813 and CA72074 (to S.J. Galli).

The authors have no conflicting financial interests.

Submitted: 7 August 2009 Accepted: 12 January 2010

REFERENCES

Alard, P., H. Niizeki, L. Hanninen, and J.W. Streilein. 1999. Local ultraviolet B irradiation impairs contact hypersensitivity induction by triggering release of tumor necrosis factor-alpha from mast cells. Involvement of mast cells and Langerhans cells in susceptibility to ultraviolet B. J. Invest. Dermatol. 113:983–990. doi:10.1046/j.1523-1747.1999.00772.x

Baroni, E., M. Biffi, F. Benigni, A. Monno, D. Carlucci, G. Carmeliet, R. Bouillon, and D. D'Ambrosio. 2007. VDR-dependent regulation of mast cell maturation mediated by 1,25-dihydroxyvitamin D3. J. Leukoc. Biol. 81:250–262. doi:10.1189/jlb.0506322

Beissert, S., A. Schwarz, and T. Schwarz. 2006. Regulatory T cells. *J. Invest. Dermatol.* 126:15–24. doi:10.1038/sj.jid.5700004

Boonstra, A., F.J. Barrat, C. Crain, V.L. Heath, H.F. Savelkoul, and A. O'Garra. 2001. 1α,25-Dihydroxyvitamin D3 has a direct effect on naive CD4+ T cells to enhance the development of Th2 cells. *J. Immunol*. 167:4974–4980.

Bouillon, R., G. Carmeliet, L. Verlinden, E. van Etten, A. Verstuyf, H.F. Luderer, L. Lieben, C. Mathieu, and M. Demay. 2008. Vitamin D and human health: lessons from vitamin D receptor null mice. *Endocr. Rev.* 29:726–776. doi:10.1210/er.2008-0004

Chervenick, P.A., and D.R. Boggs. 1969. Decreased neutrophils and megakaryocytes in anemic mice of genotype W/Wⁿ. J. Cell. Physiol. 73:25– 30. doi:10.1002/jcp.1040730104

Ellison, T.I., M.K. Smith, A.C. Gilliam, and P.N. MacDonald. 2008. Inactivation of the vitamin D receptor enhances susceptibility of murine skin to UV-induced tumorigenesis. J. Invest. Dermatol. 128:2508–2517. doi:10.1038/iid.2008.131

Galli, S.J., M. Grimbaldeston, and M. Tsai. 2008. Immunomodulatory mast cells: negative, as well as positive, regulators of immunity. Nat. Rev. Immunol. 8:478–486. doi:10.1038/nri2327

- Galli, S.J., J. Kalesnikoff, M.A. Grimbaldeston, A.M. Piliponsky, C.M. Williams, and M. Tsai. 2005. Mast cells as "tunable" effector and immunoregulatory cells: recent advances. *Annu. Rev. Immunol.* 23:749–786. doi:10.1146/annurev.immunol.21.120601.141025
- Gorman, S., L.A. Kuritzky, M.A. Judge, K.M. Dixon, J.P. McGlade, R.S. Mason, J.J. Finlay-Jones, and P.H. Hart. 2007. Topically applied 1,25-dihydroxyvitamin D3 enhances the suppressive activity of CD4+CD25+cells in the draining lymph nodes. J. Immunol. 179:6273–6283.
- Grimbaldeston, M.A., S. Nakae, J. Kalesnikoff, M. Tsai, and S.J. Galli. 2007. Mast cell-derived interleukin 10 limits skin pathology in contact dermatitis and chronic irradiation with ultraviolet B. Nat. Immunol. 8:1095–1104
- Hart, P.H., M.A. Grimbaldeston, G.J. Swift, E.K. Hosszu, and J.J. Finlay-Jones. 1999. A critical role for dermal mast cells in *cis*-urocanic acidinduced systemic suppression of contact hypersensitivity responses in mice. *Photochem. Photobiol.* 70:807–812. doi:10.1111/j.1751-1097.1999 .tb08286.x
- Hart, P.H., M.A. Grimbaldeston, G.J. Swift, A. Jaksic, F.P. Noonan, and J.J. Finlay-Jones. 1998. Dermal mast cells determine susceptibility to ultraviolet B-induced systemic suppression of contact hypersensitivity responses in mice. J. Exp. Med. 187:2045–2053. doi:10.1084/jem.187.12.2045
- Hart, P.H., S.L. Townley, M.A. Grimbaldeston, Z. Khalil, and J.J. Finlay-Jones. 2002. Mast cells, neuropeptides, histamine, and prostaglandins in UV-induced systemic immunosuppression. *Methods*. 28:79–89. doi:10.1016/S1046-2023(02)00201-3
- Kato, S., M.S. Kim, K. Yamaoka, and R. Fujiki. 2007. Mechanisms of transcriptional repression by 1,25(OH)2 vitamin D. Curr. Opin. Nephrol. Hypertens. 16:297–304. doi:10.1097/MNH.0b013e3281c55f16
- Khalil, Z., S.L. Townley, M.A. Grimbaldeston, J.J. Finlay-Jones, and P.H. Hart. 2001. cis-Urocanic acid stimulates neuropeptide release from peripheral sensory nerves. J. Invest. Dermatol. 117:886–891. doi:10.1046/j.0022-202x.2001.01466.x
- Kirnbauer, R., A. Köck, P. Neuner, E. Förster, J. Krutmann, A. Urbanski, E. Schauer, J.C. Ansel, T. Schwarz, and T.A. Luger. 1991. Regulation of epidermal cell interleukin-6 production by UV light and corticosteroids. J. Invest. Dermatol. 96:484–489. doi:10.1111/1523-1747.ep12470181
- Kligman, L.H. 1996. The hairless mouse model for photoaging. Clin. Dermatol. 14:183–195. doi:10.1016/0738-081X(95)00154-8
- Lehmann, B. 2005. The vitamin D3 pathway in human skin and its role for regulation of biological processes. *Photochem. Photobiol.* 81:1246– 1251. doi:10.1562/2005-02-02-IR-430
- Lu, L.F., E.F. Lind, D.C. Gondek, K.A. Bennett, M.W. Gleeson, K. Pino-Lagos, Z.A. Scott, A.J. Coyle, J.L. Reed, J. Van Snick, et al. 2006. Mast cells are essential intermediaries in regulatory T-cell tolerance. *Nature*. 442:997–1002.

- Melnikova, V.O., and H.N. Ananthaswamy. 2005. Cellular and molecular events leading to the development of skin cancer. *Mutat. Res.* 571:91–106.
- Metz, M., V. Lammel, B.F. Gibbs, and M. Maurer. 2006. Inflammatory murine skin responses to UV-B light are partially dependent on endothelin-1 and mast cells. Am. J. Pathol. 169:815–822. doi:10.2353/ajpath.2006.060037
- Moro, J.R., M. Iwata, and U.H. von Andriano. 2008. Vitamin effects on the immune system: vitamins A and D take centre stage. *Nat. Rev. Immunol*. 8:685–698. doi:10.1038/nri2378
- Nigrovic, P.A., D.H. Gray, T. Jones, J. Hallgren, F.C. Kuo, B. Chaletzky, M. Gurish, D. Mathis, C. Benoist, and D.M. Lee. 2008. Genetic inversion in mast cell-deficient (Wsh) mice interrupts Corin and manifests as hematopoietic and cardiac aberrancy. Am. J. Pathol. 173:1693–1701. doi:10.2353/ajpath.2008.080407
- Nishigori, C., D.B. Yarosh, S.E. Ullrich, A.A. Vink, C.D. Bucana, L. Roza, and M.L. Kripke. 1996. Evidence that DNA damage triggers interleukin 10 cytokine production in UV-irradiated murine keratinocytes. *Proc. Natl. Acad. Sci. USA*. 93:10354–10359. doi:10.1073/pnas.93.19.10354
- Noonan, F.P., and E.C. De Fabo. 1992. Immunosuppression by ultraviolet B radiation: initiation by urocanic acid. *Immunol. Today.* 13:250–254. doi:10.1016/0167-5699(92)90005-R
- Piliponsky, A.M., C.-C. Chen, M.A. Grimbaldeston, S.M. Burns-Guydish, J.W. Hardy, J. Kalesnikoff, C.H. Contag, M. Tsai, and S.J. Galli. 2010. Mast cell-derived TNF can exacerbate mortality during severe bacterial infections in C57BL/6-Kit^{W-sh/W-sh} mice. Am. J. Pathol. 176:926–938. doi:10.2353/ajpath.2010.090342
- Townley, S.L., M.A. Grimbaldeston, I. Ferguson, R.A. Rush, S.H. Zhang, X.F. Zhou, J.M. Conner, J.J. Finlay-Jones, and P.H. Hart. 2002. Nerve growth factor, neuropeptides, and mast cells in ultraviolet-B-induced systemic suppression of contact hypersensitivity responses in mice. *J. Invest. Dermatol.* 118:396–401. doi:10.1046/j.0022-202x.2001.01679.x
- van Etten, E., and C. Mathieu. 2005. Immunoregulation by 1,25-dihydroxyvitamin D3: basic concepts. *J. Steroid Biochem. Mol. Biol.* 97:93–101.
- Wolf, P., H. Maier, R.R. Müllegger, C.A. Chadwick, R. Hofmann-Wellenhof, H.P. Soyer, A. Hofer, J. Smolle, M. Horn, L. Cerroni, et al. 2000. Topical treatment with liposomes containing T4 endonuclease V protects human skin in vivo from ultraviolet-induced upregulation of interleukin-10 and tumor necrosis factor-alpha. J. Invest. Dermatol. 114:149–156. doi:10.1046/j.1523-1747.2000.00839.x
- Yamazaki, F., H. Okamoto, H. Miyauchi-Hashimoto, Y. Matsumura, T. Itoh, K. Tanaka, T. Kunisada, and T. Horio. 2004. XPA gene-deficient, SCF-transgenic mice with epidermal melanin are resistant to UV-induced carcinogenesis. J. Invest. Dermatol. 123:220–228. doi:10.1111/j.0022-202X.2004.22710.x